CATALYTIC REDUCTION OF METHYLENE BLUE BY MAGNETITE - SILICA COMPOSITE

W. M. N. WIJESUNDARA[1], T. C. JAYARUK[2*], R. D. WIJESEKERA[1]

[1]Department of Chemistry, Faculty of Science, University of Colombo, Colombo 03, Sri Lanka

[2]Faculty of Humanities and Sciences, Sri Lanka Institute of Information Technology, New Kandy Road, Malabe, Sri Lanka

Received 18th April 2022 / Accepted 11th August 2022

ABSTRACT

Iron oxide nanoparticle-based nanomaterials have well-known catalytic activity for the degradation of organic dyes in the water remediation process. The objective of this research was to synthesize iron oxide silica composite by sol-gel method and assess their applicability in wastewater treatment as a catalyst. Synthesized catalysts were characterized by FT-IR spectroscopy, X-ray diffractometry (XRD), and scanning electron microscopy (SEM). Vibration modes in FT-IR spectra show the presence of SiO_2 and Fe-O bonds. The formation of Fe_3O_4 is shown by the XRD patterns. SEM images indicate that iron oxide particles and flakes are distributed in the silica matrix. The effects of catalyst dosage, temperature, the initial concentration of methylene blue (MB), $NaBH_4$ concentration, foreign salts and ionic strength on MB degradation were studied. Maximum degradation of MB (99.89%) was obtained with an initial MB concentration of 20 mg dm^{-3}, catalyst dose of 1.0 g dm^{-3}, $NaBH_4$ concentration of 6.25 mmol dm^{-3} and at a temperature of 50 $^{\circ}$C. Common salts found in industrial wastewater such as NaCl, KCl, $CaCl_2$, and $MgCl_2$ inhibit the degradation of MB, while Na_2SO_4 enhances the degradation rate. Iron oxide helps in electron relay from BH_4^- to MB and silica tends to adsorb MB molecules and provide the proximity required for the catalytic reaction.

Keywords: Iron oxide nanoparticle, silica, methylene blue, wastewater treatment

*Corresponding author Email: charitha.t@sliit.lk;

http://orcid.org/0000-0003-0906-4441

DOI: http:://doi.org/10.4038/josuk.v15i2.8054

INTRODUCTION

Water is one of the most important natural resources in the world and is vital for the survival of all living beings. Along with the acceleration of industrialization and urbanization, water consumption is rapidly increasing, and water scarcity has become an issue of great concern. Water that has been adversely affected in quality by pollutants is named wastewater (Abdel-raouf et al., 2019). Organic dyes are widely used in textile, plastic, medicine and many other industries. They are not readily degradable and are typically not removed from water by wastewater treatment systems and conventional methods such as ultra-filtration, and chemical and electrochemical methods (Sharif et al., 2019). The catalytic degradation of organic dyes by nanoparticles, over the conventional methods in wastewater treatment, is an effective and rapid technique. Iron oxide nanoparticle-based nanomaterials are more attractive for removing organic dyes in the water remediation process due to their important physiochemical properties, simple regeneration ability and low cost. Iron oxide nanoparticles are more susceptible to air oxidation because of their high chemical activity on the surface (Dave & Chopda, 2014). Therefore, several materials such as polymer silica and carbon are used for surface modification and functionalization strategies of iron oxide. Silica is an excellent supporting material because of its large surface area, cost-effectiveness, high mass exchange characteristics and excellent mechanical resistance (Nikmah et al., 2019). The source of the silica is obtained from rice straw (RS), a cheap, eco-friendly, silica-rich agricultural waste material. The effects of nanocatalyst dosage, temperature, initial concentration of MB, $NaBH_4$ concentration, foreign salts and ionic strength on the catalytic performance of the Fe_3O_4-SiO_2 composite, in the degradation of MB, were investigated.

METHODOLOGY

Rice straw was collected from a paddy field in Gampaha, Sri Lanka. Ethyl alcohol (95%) was purchased from Sigma Aldrich, HCl (35.4 %), H_2SO_4 (98%), NaCl (98 %), and

KCl (98 %) were procured from Techno Pharmachem, India, $FeCl_3$ (98%) was obtained from HIMEDIA, India. Na_2SO_4 (98%) was procured from LOBA CHEMIE, India, $MgCl_2$ (98%) and NaOH (98%) were purchased from MERCK, India. $CaCl_2$ (100%) was obtained from SRL Chem, India. $NaBH_4$ (98%) was obtained from Sisco research laboratories (Pvt) Ltd, India. Methylene Blue (97%) was obtained from DAEJUNG, Korea. Distilled water was used for all experiments.

Synthesis: RS was washed with tap water, distilled water and ethanol, respectively. The washed RS was oven dried at 100 ^{0}C for 6 hours and then refluxed in 10% HCl at 70 ^{0}C for 6 hours. The resulting RS was washed with distilled water until a neutral pH was reached. RS was dried at 100 ^{0}C for 6 hours followed by calcination at 600 ^{0}C for 5 hours in an open vessel in a muffle furnace. Silica was refluxed in 3.0 M NaOH solution at 70 ^{0}C for 4 hours. The resulting sodium silicate solution was filtered to remove any impurities. A quantity of $FeCl_3$ was weighed where moles of Fe^{3+} are half the synthesized silica moles. The prepared Fe^{3+} solution was added dropwise to the sodium silicate solution while stirring. The resulting solution was stirred continuously for 3 hours. Thereafter, 0.5 M sulfuric acid was added dropwise into the suspension to initiate the hydrolysis-condensation reaction and addition was continued until the pH reached 4. The resulting suspension was stirred for 4 hours continuously. The suspension was centrifuged at 3000 rpm for 10 min followed by washing with distilled water under sonication for another 10 min. The steps of centrifugation and sonication were repeated several times until a neutral pH was achieved and SO_4^{2-} ions were removed entirely. The final product consisted of two types of precipitates, brown colour (BCN) and dark brown colour (DBCN) composites. Composites were separated manually depending on the colour difference and dried at 100 ^{0}C for 24 hours.

Characterization: The morphology of the prepared BCN and DBCN was characterized using a scanning electron microscope (EVO 18) coupled with an energy dispersive X-ray

analyser (EDX). X-ray diffraction (XRD) patterns were collected by using a BRUKER D8 ADVANCE ECO X-ray diffractometer with diffraction angle 2θ between 5° and 80° using Cu-Kα radiation of wavelength 1.54 Å to determine crystal phase. Functional groups were identified using a FTIR spectrophotometer (Spectrum Two-95033). The absorbance of methylene blue was measured by a UV-Vis spectrophotometer (GENESYS 10S). A pH meter (HI 2211) was used to measure the pH of all solutions.

Catalytic Degradation of MB: A typical reaction mixture contained 50 ml of 40 mg dm^{-3} MB solution (C_0) and 0.31 mmol of $NaBH_4$. Catalyst (50 mg) was added to the MB solution, while magnetically stirring at 500 rpm. At given reaction time intervals, 2 ml aliquots were withdrawn and the absorbance of MB (C_t) was measured. For the determination of MB concentration, after appropriate dilution, the aliquots withdrawn were centrifuged at 3000 rpm for 5 min followed by subsequent UV–Vis analysis of the supernatant solutions. The MB concentration was determined based on the constructed calibration curve at the maximum absorption wavelength (λ_{max}) of 664 nm. This experiment was performed by using both BCN and DBCN separately. Control experiments were carried out to verify the catalytic efficiency of the synthesized composites by using a reaction mixture containing only MB, only the BCN, only the DBCN and only $NaBH_4$ under the same experimental conditions. All batch experiments were conducted at room temperature, with an initial pH of 6 and NaBH4 concentration of 6.25 mmol dm-3, 1.0 g dm-3 catalyst dosage, and an initial MB concentration of 40 ppm. The nanocomposite containing the highest degradation efficiency was used in further dye degradation experiments. The influence of MB concentration (20 - 160 ppm), $NaBH_4$ concentration (2.64 – 100 mmol dm^{-3}), catalyst dosage (0.25, 0.5, 1.0 g dm^{-3}), reaction temperature (303, 313, 323 K), foreign salts and ionic strength on MB degradation were studied. The MB degradation efficiency (E) at 5 minutes was calculated as follows.

$$E = \frac{C_0 - C_t}{C_t} \times 100 \qquad (1)$$

Kinetic Study: The rate of MB degradation by nano metallic particles was studied by a pseudo-first-order reaction model within the first 10 minutes.

$$\ln\left(\frac{C_t}{C_0}\right) = -kt \qquad (2)$$

Where C_0 represents the original concentration of MB (mg/L), C_t is the residual concentration of MB at time t (minutes), and k is the pseudo-first-order rate constant (min^{-1}).

RESULTS AND DISCUSSION

The FTIR spectra of the synthesized composites were acquired in the range of 400-4500 cm^{-1}. FTIR spectra of BCN and DBCN are presented in Figures 1 (a) and (b), respectively. The peak at 585 cm^{-1} is assigned to the characteristic Fe–O vibration, while the peak at 543 cm^{-1} is ascribed to the vibration of the Si-O-Fe bond (Kokate et al., 2013). The band at 1095 cm^{-1} is assigned to Si-O-Si stretching and the band at 786 cm^{-1} to Si-O bending The FTIR spectra of the synthesized composites were acquired in the range of 400-4500 vibrations. The presence of two distinct bands at 959 cm^{-1} and 1633 cm^{-1} are ascribed to Si-O stretching vibration. The broad absorbance peak at 3366 cm^{-1} is attributed to the O-H bond vibration of absorbed water molecules and silanol groups (Si-OH) (Maurice & Faouzi, 2014). Both BCN and DBCN composites have these common characteristic peaks suggesting the presence of an oxide of iron on a silica matrix.

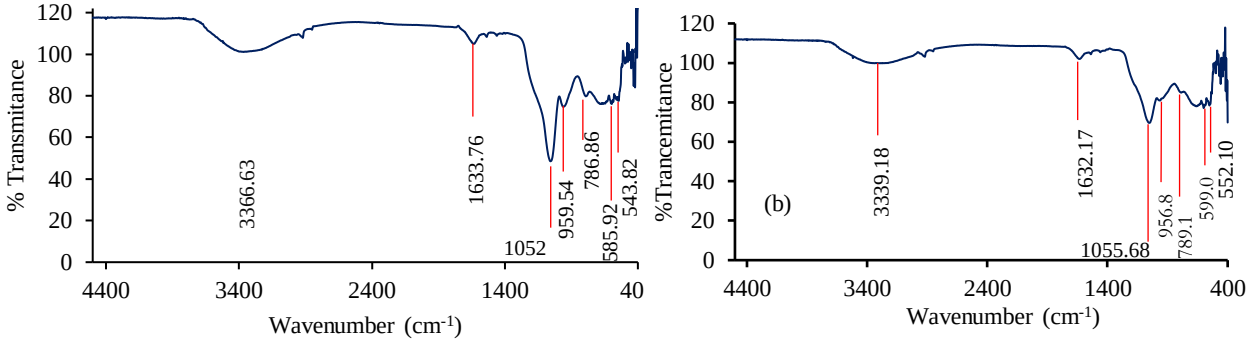

Figure 1. FTIR spectrum of (a) BCN (b) DBCN

Figures 2 (a) and (b) show the XRD patterns of BCN and DBCN, respectively. The peak at 35.6° in the XRD pattern shown in Figure 2 (a) corresponds to the (311) plane of Fe_3O_4 (113). The broad peak centered at 22.3° indicates the presence of amorphous SiO_2 (Tari et al., 2017). However, the weak diffraction peaks in Figures 2 (a) and (b) were due to the low crystallinity of iron oxide as they were heated only to 100 °C.

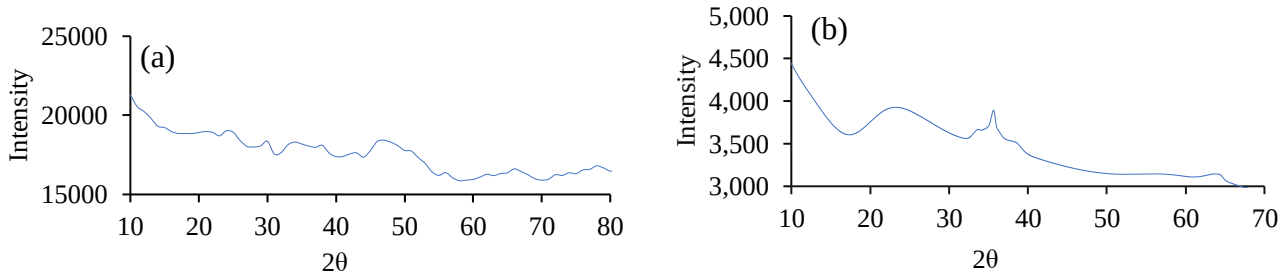

Figure 2. XRD patterns of (a) BCN (b) DBCN

SEM images shown in Figures 3 (a) and (b), acquired using a SEI detector show that both BCN and DBCN consist of aggregated spherical and irregular-shaped particles of different sizes, in the range of 100 to 200 nm. Primary particles showed a tendency to aggregate and form clusters of larger particles. Aggregation could result from rapid nucleation due to the higher surface energy and free OH groups of the silica surface resulting in the formation of hydrogen bonds with water molecules and particle each other, resulting

in large particle with agglomeration (Azlina et al., 2016). Images shown in Figures 3 (c) and (d) were collected by the BSD detector. Figure 3 (d) shows that iron oxide plates of thickness in the nano range are present in DBCN but not in BCN. Therefore, the weight of DBCN is higher than that of BCN, resulting in a darker brown colour. The EDX results of BCN and DBCN show mainly the presence of iron, oxygen, and c. The presence of sulphur in minor concentrations may be due to the incomplete wash-off of sulfuric acid used in the synthesis.

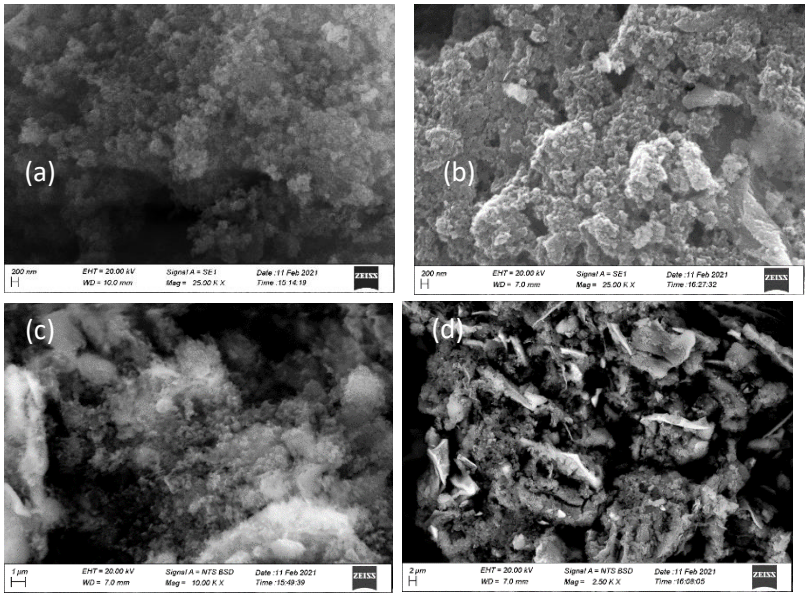

Figure 3. SEM images of a) BCN b) DBCN using SE1 detector, c) BCN d) DBCN using BSD detector

Degradation of MB using $NaBH_4$ Alone, BCN alone, DBCN alone, BCN with $NaBH_4$ and DBCN with $NaBH_4$: According to the results in Figure 4, the absorbance at 664 nm decreased with increasing time and disappeared after 20 min, indicating the complete degradation of MB molecules. No noticeable decolourization was observed for MB solution with only $NaBH_4$. On the other hand, the reaction mixture containing MB in the presence of Fe_3O_4-SiO_2 did not show any further decrease in MB concentration after establishing adsorption/desorption equilibrium. Hence, the ratio of C_t/C_0 remains almost unchanged during the reaction. Based on the results, BCN has a higher adsorption capacity than DBCN due to its higher content of silica. Negatively charged silanol groups on BCN facilitate the

adsorption of positively charged MB molecules. Thus, dye degradation efficiency and rate in the presence of $NaBH_4$ are comparatively higher in BCN than in DBCN. Therefore, BCN was selected for further studies.

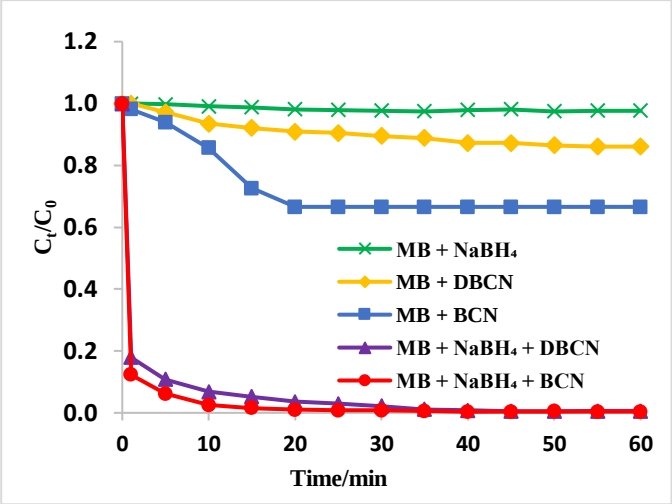

Figure 4. MB degradation with BCN, DBCN and $NaBH_4$ as a function of reaction time

Effect of MB concentration on the degradation of MB BCN and DBCN: To investigate the influence of the initial dye concentration on catalytic degradation of MB, different concentrations of MB (20, 40, 80 and 160 ppm) were used with 6.25 mmol dm^{-3} of $NaBH_4$, and 1.0 g dm^{-3} catalyst dosage. The degradation efficiency of MB decreased with increasing concentration of MB. Percentage degradation of 99.89 % which was obtained with 20 mg dm^{-3} of 95% dropped to 40.44 % with 160 mg dm^{-3} in a reaction time of 5 minutes. The rate constant for degradation of MB decreased from 0.519 min^{-1} to 0.072 min^{-1} when the concentration of MB increased from 20 mg dm^{-3} to 160 mg dm^{-3} as shown in the insert of Figure 5. The number of active sites is the limiting factor that determines the rate of degradation with increasing MB concentration. Active sites occupied by the MB molecules would be vacant for the other MB molecules in the solutions to adsorb onto, only after the degradation of the existing molecules. Further, the porous structure of the catalyst is clogged by bulky MB molecules at higher concentrations limiting the adsorbent surface. The catalyst

links the reactants, and the electrons transfer process from the reducing agent to MB molecules decreases. Hence, the rate of catalytic degradation of MB decreases with increasing MB concentration.

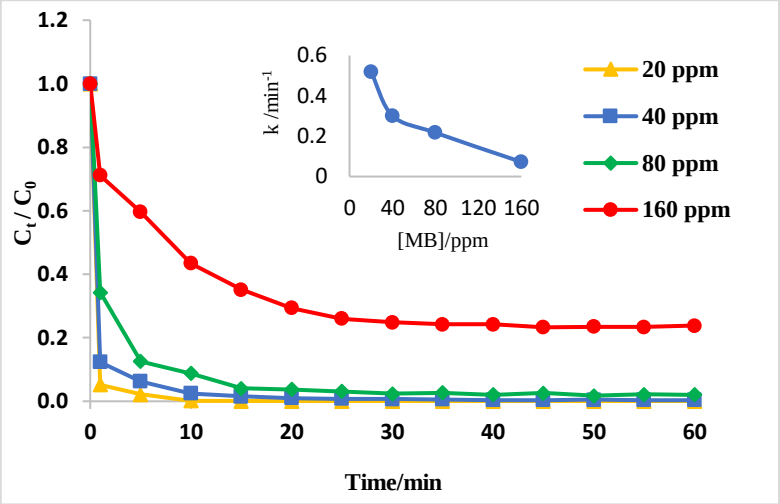

Figure 5. Effect of initial MB concentration on the degradation of MB with 6.25 mmol dm^{-3} of $NaBH_4$, and 1.0 g dm^{-3} catalyst dosage. Insert – Variation of the rate constant with varying MB concentration

Effect of $NaBH_4$ concentration on the degradation of MB: The reductant concentration played an important role related to the number of BH_4^- ion concentrations during the degradation process. The results depicted in Figure 6 indicate that the MB removal rate increased as the initial $NaBH_4$ concentration increased from 2.64 to 6.25 mmol dm^{-3}. The degradation efficiency increased from 90.70 % to 93.78 % at 5 minutes. This was because a sufficient number of BH_4^- ions were generated in the electron transfer process at higher $NaBH_4$ concentrations, which was beneficial to the degradation of MB. However, the efficiency and the rate of MB degradation decreased when $NaBH_4$ concentration was further increased to 50 mmol dm^{-3}.

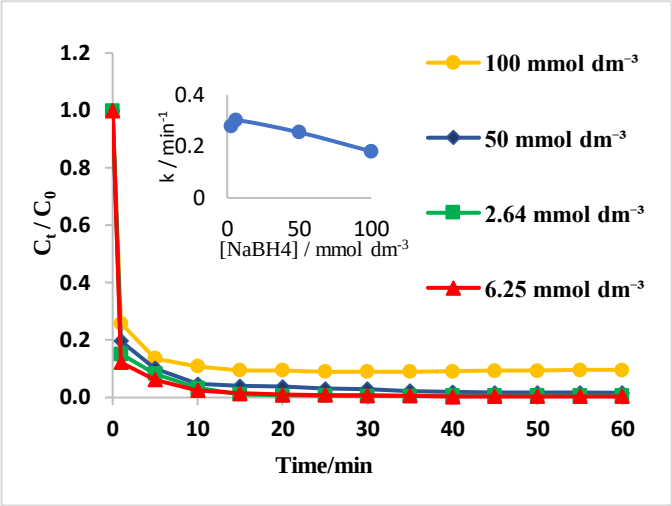

Figure 6. Effect of initial $NaBH_4$ concentration on the degradation of MB with 40 ppm of MB, and 1.0 g dm^{-3} catalyst dosage. Insert – Variation of the rate constant with varying MB concentration

The inset in Figure 6 shows that the k value initially increased to 0.302 min^{-1} and then decreased as the concentration continued to increase to 50 mmol dm^{-3} and degradation efficiency decreased to 89.78 %. When the $NaBH_4$ concentration exceeds the critical level, excess NaBH4 would react with water molecules and produced many hydrogen gas bubbles hindering the movement of MB towards the surface of the catalyst. Furthermore, adsorbed MB molecules would be desorbed. Thus, the rate of reaction and degradation efficiency decreases with increasing $NaBH_4$ concentration. Therefore, the optimum decolouration efficiency and degradation rate were achieved at 6.25 mmol dm^{-3} NaBH4 concentration. BH_4^- ions acted as the reducing agent and methylene blue was converted to colorless Leuco Methylene blue (LMB).

Effect of catalyst dosage on the degradation of MB: The dosage of Fe_3O_4-SiO_2 was another vital parameter affecting the removal efficiency. According to the results shown in Figure 6, when the catalyst dosage increased from 0.25 to 1.0 g dm^{-3}, the dye degradation rate increased significantly. Figure 7 shows that the k value increased with increasing

catalytic dosage. This is due to the greater number of active sites available due to the increased surface area, on increasing the composite dosage, favouring the adsorption of MB and $NaBH_4$. A MB degradation efficiency of nearly 93.78 % was achieved at a reaction time of 5 min with a dose of 1.0 g dm^{-3}, while 37.50 % was obtained with a catalyst dosage of 0.25 g dm^{-3}.

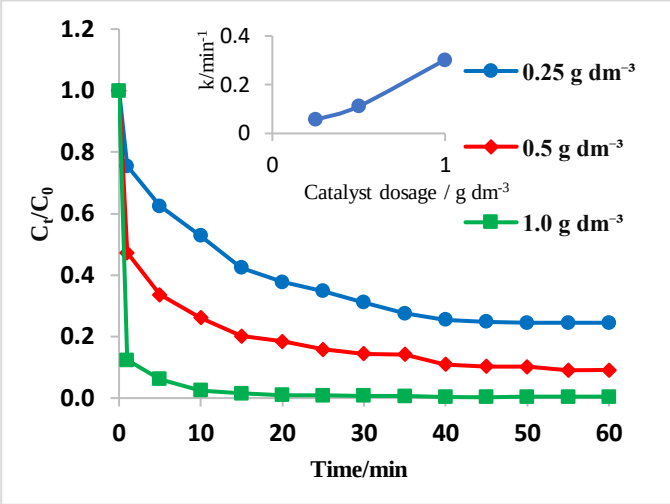

Figure 7. Effect of BCN catalyst dosage on the degradation of MB with 40 ppm of MB, and 1.0 g dm^{-3} catalyst dosage and 6.25 mmol dm^{-3} of $NaBH_4$. Insert – Variation of the rate constant with varying MB concentration

Effect of temperature on the degradation of MB: The effect of temperature on the degradation of MB is shown in Figure 8. The MB degradation efficiency increased from 93.78 to 97.90% and the rate constant for the degradation increased from 0.302 to 0.356 min^{-1} on increasing the temperature of the medium from 303 to 323 K. High temperatures lead to a higher collision frequency between BH_4^- ions and MB, resulting in a rapid degradation rate. In addition, MB diffuses rapidly through the dye solution to the surface or the pores of the material and interacts effectively with the adsorption sites at higher temperatures (Liu et al., 2019).

The Arrhenius equation is given below:

$$\ln k = -\frac{E_a}{RT} + \ln A_0 \quad (3)$$

Where A_0 is the pre-exponential factor, E_a is the Arrhenius activation energy (kJ/ mol), R is the universal gas constant (8.314 J/mol K), and T is the temperature (K). The Arrhenius plot of ln k against 1/T is presented in Figure 9. From the slope of the Arrhenius plot, E_a/R, the activation energy was calculated to be 6.77 kJ/mol under these experimental conditions.

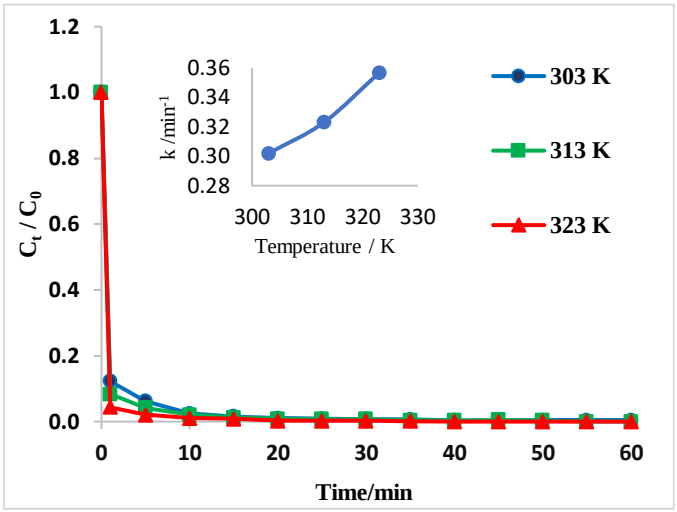

Figure 8. Effect of temperature on the degradation of MB with 40 ppm of MB, and 1.0 g dm^{-3} catalyst dosage and 6.25 mmol dm^{-3} of $NaBH_4$. Insert – Variation of the rate constant with varying MB concentration

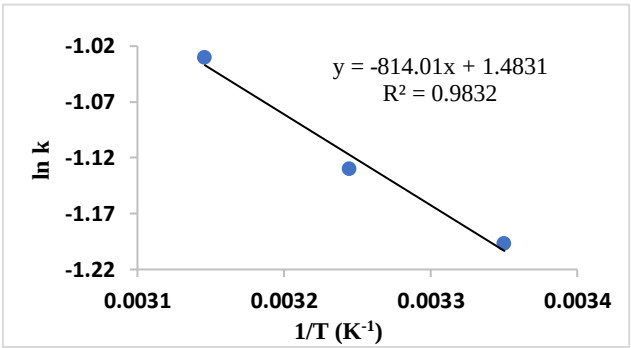

Figure 9. Corresponding Arrhenius plot

Effect of foreign salts and ionic strength on the degradation of MB: The effect of foreign salts on the degradation of MB was studied for this Fe_3O_4-SiO_2/$NaBH_4$ system. The results obtained are depicted in Figure 10. As shown in the figure, the degradation efficiency and the rate constant for degradation of MB (40 mg dm^{-3}) decline in 0.01 M of NaCl (93.44 % and 0.282 min^{-1}), KCl (89.56 % and 0.207 min^{-1}), $MgCl_2$ (83.39 % and 0.143 min^{-1}) and $CaCl_2$ (68.09 % and 0.0945 min^{-1}). However, with Na_2SO_4, the degradation efficiency and rate constant were 97.73 and 0.334 min^{-1} respectively, which is greater than that obtained when no salts were added (control sample). To further identify the effect of ionic strength on the removal of MB, solutions of varying ionic strengths (0.01, 0.1 and 1.0 M) of NaCl were used. As shown in Figure 11, the MB degradation rate and efficiency decreased as the ionic strength increased from 0.01 M (93.44 %) to 1.0 M (63.56 %). The inset in Figure 10 shows that k decreases gradually with increasing NaCl concentration.

When ionic strength is increased, positively charged Na^+ ions occupy on the negatively charged sites of the catalyst surface. Hence, there were no more negatively charged sites available for the adsorption of positively charged MB dye, lowering the degradation rate and efficiency. However, when compared to the control sample, the degradation rate and the efficiency in Na_2SO_4 containing medium increased because, the presence of the divalent sulphate anion could be attributed to its higher valency, in which a stronger electrostatic field could be more efficient in reducing the electrostatic repulsion barrier between MB molecules and catalytic surface by neutralizing positive sites of Fe^{3+}. As a result, non-electrostatic interactions such as low energetic H-bonds or van der Waals short-ranged interactions can occur between cationic MB and the neutral site. Divalent cations such as Mg^{2+} and Ca^{2+} have slowed down the degradation process to a greater extent than monovalent cations such as K^+ and Na^+. This implies that multivalent cations with stronger electrostatic attraction to the negative silica surface are more efficient in competing

with MB molecules for adsorption on the catalyst surface (Gan & Li, 2013). In addition, the rate of degradation and efficiency decrease as the hydrated ionic radii of the added foreign cations of the same valency decrease as follows: K^+ (3.31 Å) < Na^+ (3.58 Å); Ca^{2+} (4.12 Å) < Mg^{2+} (4.28 Å) (Dove & Nix, 1997). The greater the ion's hydration, the farther it is from the adsorbing surfaces, hence the weaker its adsorption. Thus, cations with greater hydrated ionic radii would be less efficient at competing with the cationic MB for the adsorption sites on the catalyst surface resulting in a higher rate of MB degradation.

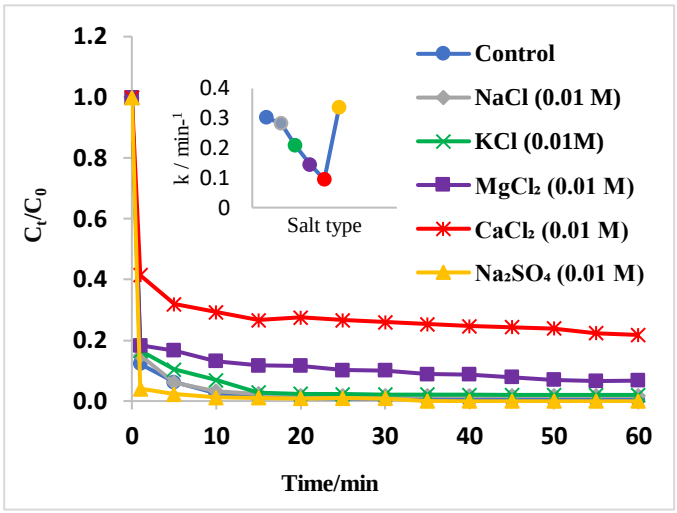

Figure 10. Effect of various foreign salts on the MB degradation and variation of the rate constant

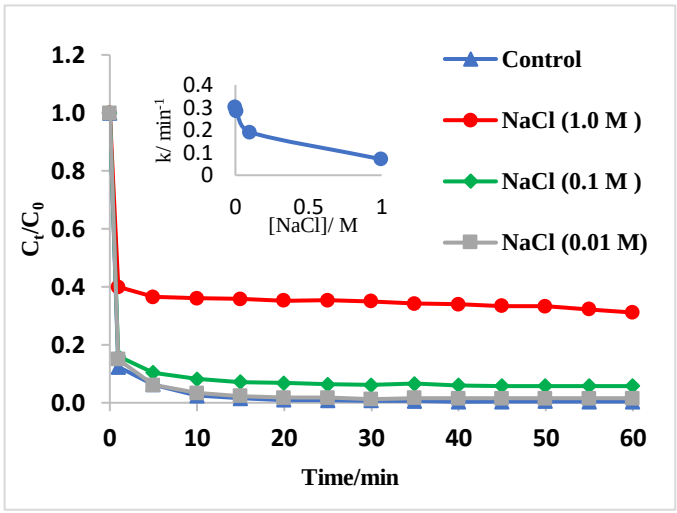

Figure 11. Effect of ionic strength on the MB degradation efficiency at 5 minutes and variation of the rate constant

Table 1 compares the rate/conversion of MB with respect to the data reported in the literature. It can be seen that the synthesized composite in this study is more effective than what is reported in the literature which could be due to the presence of silica matrix which enhances the adsorption of MB molecules because when the reactant molecules are proxime to the catalyst the reduction reaction is further enhanced.

Table 1. A comparison of the activity of the nanomaterial on catalytic degradation of MB

Catalyst	Concentration of MB (ppm)	Weight/volume of the catalyst	Concentration of $NaBH_4$ (mol dm^{-3})	Conversion /Rate	Time taken	Reference
Silver nanoparticles	10	1 mL	0.2	34.74 %	6 min	(Fairuzi et al., 2018)
Gold nanoparticles	1	-	10×10^{-3}	0.241 min^{-1}	9 min	(Ganapuram et al., 2015)
Silver nanoparticles	50×10^{-3}	0.05	5×10^{-3}	0.106 min^{-1}	20	(Somasundaram et al., 2021)
Fe_3O_4/SiO_2	40	50 mg	6.25×10^{-3}	0.52 min^{-1}	5 min	This study

CONCLUSION

In this study, an iron oxide nanoparticle-nanosilica composite was prepared successfully using low-cost and abundant rice straw waste. The catalytic effect of both BCN and DBCN was evaluated on the degradation of MB using $NaBH_4$ as the catalyst. BCN is more catalytically active than DBCN due to the high weight proportion of silica, which facilitates the MB adsorption that enhances the catalytic activity. The MB degradation rate was improved with an increase in the dosage of the catalyst, the concentration of $NaBH_4$,

and pH (up to a certain limit). However, the degradation rate decreased as the initial MB concentration was increased. The optimum conditions for MB degradation were as follows: an initial MB concentration of 20 mg dm^{-3}, a catalyst dose of 1.0 g dm^{-3}, 6.25 mmol dm^{-3} of $NaBH_4$, and a temperature of 50 ^oC. The highest removal rate of MB was found to be 99.89 % with an initial MB concentration of 20 mg dm^{-3}, followed by 93.78 % with an initial MB concentration of 40 mg dm^{-3} at 5 minutes. The study on the effect of foreign salts and ionic strength shows that when ionic strength is increased, the degradation rate of MB gradually decreases and the salts such as Na_2SO_4 could actually enhance the degradation rate and efficiency.

REFERENCES

Abdel-raouf, M. E., Maysour, N. E., & Farag, R. K. (2019). Wastewater Treatment Methodologies , Review Article International Journal of Environment & Agricultural Science Wastewater Treatment Methodologies , Review Article. *International Journal of Environment & Agricultural Science*, *January*, 1–2.

Azlina, H. N., Hasnidawani, J. N., Norita, H., & Surip, S. N. (2016). Synthesis of SiO2 nanostructures using sol-gel method. *Acta Physica Polonica A*, *129*(4), 842–844. https://doi.org/10.12693/APhysPolA.129.842

Dave, P. N., & Chopda, L. V. (2014). Application of iron oxide nanomaterials for the removal of heavy metals. *Journal of Nanotechnology*, *2014*, 1–2. https://doi.org/10.1155/2014/398569

Dove, P. M., & Nix, C. J. (1997). magnesium, calcium, and barium on the dissolution kinetics of quartzThe influence of the alkaline earth cations,. *Geochimica et Cosmochimica Acta*, *61*(16), 3329–3340. https://doi.org/10.1016/S0016-7037(97)00217-2

Fairuzi, A. A., Bonnia, N. N., Akhir, R. M., Abrani, M. A., & Akil, H. M. (2018).

Degradation of methylene blue using silver nanoparticles synthesized from imperata cylindrica aqueous extract. *IOP Conference Series: Earth and Environmental Science*, *105*(1), 12018.

Gan, P. P., & Li, S. F. Y. removal of R. B. using a rice hull-based silica supported iron catalyst by F. process. (2013). Efficient removal of Rhodamine B using a rice hull-based silica supported iron catalyst by Fenton-like process. *Chemical Engineering Journal*, *229*, 359–360. https://doi.org/10.1016/j.cej.2013.06.020

Ganapuram, B. R., Alle, M., Dadigala, R., Dasari, A., Maragoni, V., & Guttena, V. (2015). Catalytic reduction of methylene blue and Congo red dyes using green synthesized gold nanoparticles capped by salmalia malabarica gum. *International Nano Letters 2015 5:4*, *5*(4), 215–222. https://doi.org/10.1007/S40089-015-0158-3

Kokate, M., Garadkar, K., & Gole, A. (2013). One pot synthesis of magnetite-silica nanocomposites: Applications as tags, entrapment matrix and in water purification. *Journal of Materials Chemistry A*, *1*(6), 2022–2026. https://doi.org/10.1039/c2ta00951j

Liu, J., Du, Y., Sun, W., Chang, Q., & Peng, C. (2019). Preparation of new adsorbent-supported Fe/Ni particles for the removal of crystal violet and methylene blue by a heterogeneous Fenton-like reaction. *RSC Advances*, *9*(39), 22513–22522. https://doi.org/10.1039/c9ra04710g

Maurice, A. R., & Faouzi, H. (2014). Synthesis and Characterization of Amorphous Silica Nanoparitcles from Aqueous Silicates Uisng Cationic Surfactants. *Journal of Metals, Materials and Minerals*, *24*(1), 37–42.

Nikmah, A., Taufiq, A., & Hidayat, A. (2019). Synthesis and Characterization of Fe3O4/SiO2 nanocomposites. *IOP Conference Series: Earth and Environmental Science*, *276*(1), 1–6. https://doi.org/10.1088/1755-1315/276/1/012046

Sharif, H. M. A., Mahmood, A., Cheng, H. Y., Djellabi, R., Ali, J., Jiang, W. L., Wang, S. Sen, Haider, M. R., Mahmood, N., & Wang, A. J. (2019). Fe3O4 Nanoparticles Coated with EDTA and Ag Nanoparticles for the Catalytic Reduction of Organic Dyes from Wastewater. *ACS Applied Nano Materials*, *2*(8), 1–2. https://doi.org/10.1021/acsanm.9b01250

Somasundaram, C. K., Atchudan, R., Edison, T. N. J. I., Perumal, S., Vinodh, R., Sundramoorthy, A. K., Babu, R. S., Alagan, M., & Lee, Y. R. (2021). Sustainable synthesis of silver nanoparticles using marine algae for catalytic degradation of methylene blue. *Catalysts*, *11*(11), 1377. https://doi.org/10.3390/CATAL11111377/S1

Tari, F., Shekarriz, M., Zarrinpashne, S., & Ruzbehani, A. (2017). Synthesis, characterization, and optimization of α-Fe2O3/silica nanocomposites using homogenous precipitation method. *International Journal of Applied Ceramic Technology*, *14*(4), 7–8. https://doi.org/10.1111/ijac.12684